Chemical Engineering Journal 152 (2009) 376–388

Contents lists available at ScienceDirect

Chemical Engineering Journal

journal homepage: www.elsevier.com/locate/cej

Competitive sorption of lead and cadmium onto sediments

Sanghwa Oh, Moon Yong Kwak, Won Sik Shin*

Department of Environmental Engineering, Kyungpook National University, Daegu 702-701, Republic of Korea

ARTICLE INFO

Article history:
Received 23 January 2009
Received in revised form 16 April 2009
Accepted 28 April 2009

Keywords:
Sorption
Cadmium (Cd)
Competition
Competitive Langmuir model (CLM)
Ideal adsorbed solution theory (IAST)
Langmuir model
Lead (Pb)
Sediment

ABSTRACT

Single- and bi-solute competitive sorptions of Pb and Cd onto sediments were investigated. In single-solute sorption, Khan model was fitting better than the other models such as Freundlich, Langmuir, Dubinin–Radushkevich, Sips, Redlich–Peterson and Kargi–Ozmıhcı models. In bi-solute sorption, competition between the solutes reduced the sorbed amount of each solute compared with that in the single-solute system. Langmuir model parameters for single-solute (q_{mL} and b_L) and bi-solute (q^*_{mL} and b^*_L) competitive sorptions were compared. Sediment with higher pH, CEC and BET surface area had higher maximum sorption capacity (q_{mL}). In all sediments, maximum sorption capacity (q_{mL}) of Pb was higher than that of Cd, and the presence of both metals reduced the tendency to be sorbed although Cd sorption was more affected than Pb. The b^*_L values of Pb decreased while those of Cd increased indicating that competition for sorption sites promotes the retention of Cd on more specific sorption sites. The competitive Langmuir model (CLM) and ideal adsorbed solution theory (IAST) coupled to the single-solute sorption models predicted Pb sorption in bi-solute competitive sorption favorably but not Cd sorption.

1. Introduction

Lead and cadmium from anthropogenic sources have been one of the most significant problems because of their toxicity, persistence, and non-biodegradable nature [1]. These metals are particularly toxic to higher animals, producing kidney and blood diseases among other health disorders [2]. Lead and cadmium can be sorbed onto sediments and released again under certain conditions. Therefore, sediments have become the main sink and source of heavy metals like Pb and Cd in river and marine environment. The physicochemical characteristics of the sediments, such as the amount of organic and inorganic matter, redox potential, pH, and oxygen, affect the mobility of sediment-bound metals [3].

Heavy metals such as Pb and Cd in aquatic systems are easily sorbed on sediments. The metal sorption depends on the sediment characteristics, characteristics of involved metals, and their competition for sorption sites on sediments, which are affected by pH. Christensen [4] reported that the sorption capacity of soils and sediments for Cd increased two to three times for a pH increase of one unit and the sorption for Cd was predominant process at pH 6. The sorption intensity and capacity of sediments for metals are also affected by a variety of sediments substrates such as clay, metal oxides, and organic compounds while the composition and structure of natural sediments are extremely site-specific [5]. The heavy metals are distributed among the different components of sediments in real environments and variations in the chemical composition of sediments may further affect the partitioning of metals into sorbent [6]. In several studies, Pb, Cu and Cr are more strongly retained in soils and minerals than Zn, Ni and Cd in competitive sorption conditions [7–13]. For sediments, however, little information for competitive sorption is available [14]. Although some researchers reported that Pb sorption onto sediments was higher than Cd under the competitive conditions [3,15–17], further studies are needed to provide more valuable information on competitive sorption mechanisms in sediments.

The competitive sorption model can simulate the sorption process of metals at particle surfaces if sorption is the major process under unsaturated condition [18]. The ideal adsorbed solution theory (IAST) has the advantages that no mixture data are required and no restriction exists for the type of pure-component isotherm equation [19], but IAST can make erroneous predictions caused by a large difference in molecular size and adsorbent heterogeneity [20]. To overcome this drawback, many studies on IAST have been carried out [10,21–25]. Although several thermodynamic competitive sorption models such as ideal adsorbed solution theory (IAST) and competitive Langmuir model (CLM) have been used for understanding and predicting competitive sorption of multi-solutes, little information is currently available for sediments.

In this paper, single- and bi-solute sorption experiments of Pb and Cd onto natural sediments with different characteristics were carried out in a batch-type adsorber. Single-solute sorption data were analyzed using several sorption models: Freundlich,

---

* Corresponding author at: Department of Environmental Engineering, Kyungpook National University, 1370 Sankyuk-Dong, Buk-Gu, Daegu 702-701, Republic of Korea. Tel.: +82 53 950 7584; fax: +82 53 950 6579.

E-mail address: wshin@mail.knu.ac.kr (W.S. Shin).

1385-8947/$ – see front matter © 2009 Elsevier B.V. All rights reserved.
doi:10.1016/j.cej.2009.04.061

Nomenclature

b_K	Khan model constant (L/mmol)
b_L	Langmuir model constant (L/mmol)
$b_{L,i}$	Langmuir model constant for solute *i* (L/mmol)
b_R	Redlich–Peterson model constant $(\mathrm{L/mmol})^{N_R}$
b_S	Sips model constant (L/mmol)
C	aqueous-phase equilibrium concentration (mmol/L)
$C_{m,i}$	aqueous-phase equilibrium concentration of a solute *i* in a mixture (mmol/L)
C_i^*	equilibrium concentration of a solute *i* sorbed singly at the same condition as a mixture (mmol/L)
CLM	competitive Langmuir model
E	mean free energy (J/mol) in Dubinin–Radushkevich model
IAST	ideal adsorbed solution theory
K_F	Freundlich sorption coefficient $(\mathrm{mmol/g})/(\mathrm{mmol/L})^{N_F}$
K_G	Kargi–Ozmıhcı saturation constant (mmol/L)
N	total number of solutes in a mixture
N_F	exponent in Freundlich model
N_G	exponent in Kargi–Ozmıhcı model
N_K	exponent in Khan model
N_R	exponent in Redlich–Peterson model
N_S	exponent in Sips model
q	solid-phase equilibrium concentration (mmol/g)
q_i^*	solid-phase equilibrium concentration of a solute *i* sorbed singly at the same condition as a mixture (mmol/L)
$q_{m,i}$	solid-phase equilibrium concentration of a solute *i* in an sorbent (mmol/g)
q_{mD}	maximum sorption capacity in Dubinin–Radushkevich model (mmol/g)
q_{mG}	maximum sorption capacity in Kargi–Ozmıhcı model (mmol/g)
q_{mK}	maximum sorption capacity in Khan model (mmol/g)
q_{mL}	maximum sorption capacity in Langmuir model (mmol/g)
$q_{mL,i}$	maximum sorption capacity for solute *i* in Langmuir model (mmol/g)
q_{mR}	maximum sorption capacity in Redlich–Peterson model (mmol/g)
q_{mS}	maximum sorption capacity in Sips model (mmol/g)
q_T	total sorbed concentration of all solute in the mixture (mmol/g)
R	gas constant, 8.314 (J/mole/K)
SSE	sum of square errors
T	absolute temperature (K)
V	solution volume (L)
W	sorbent weight (g)
z_i	mole fraction of solute *i* in the sorbed phase
Greek letters	
β	Dubinin–Radushkevich model parameter $(\mathrm{mol}^2/\mathrm{J}^2)$
ε	Polanyi potential (J/mol)

Langmuir, Dubinin–Radushkevich, Sips, Redlich–Peterson, Kargi–Ozmıhci and Khan models. Langmuir model parameters for single- (q_{mL} and b_L) and bi-solute (q_{mL}^* and b_L^*) competitive sorptions were compared to analyze the effect of competition. Bi-solute competitive sorption data were compared with the predictions from the competitive Langmuir model (CLM) and the ideal adsorbed solution theory (IAST) coupled to the single-solute sorption models.

2. Materials and methods

2.1. Materials

Three sediment samples were collected from the surface layer (0–20 cm) of coastal sediments in Buan (Sediment A) and Suncheon, Korea (Sediment B and C). The sediment samples were air-dried and passed through a 200-mesh sieve, homogenized and stored in a plastic bottle until use. Some basic physicochemical properties of the sediments are listed in Table 1. Sediment pH was measured using a pH meter (Orion 290A) at sediment to solution ratio of 1:2.5 (w/v) in deionized water. Organic carbon content was determined by an elemental analyzer (Fisons, EA 1110/EA1108) after removal of inorganic carbon. Cation exchange capacity (CEC) was determined by the Sodium Acetate Method (U.S. EPA Method 9081) [26]. The mineralogical compositions of the sediments were identified by an X-ray diffractometer (Rigaku, D/Max-IC) (Fig. 1 and Table 1). The background concentrations of Pb and Cd in the sediment were measured by microwave acid digestion (U.S. EPA Method 3051) [27]. Sediment samples (1.0 g) were digested with 2 mL of HNO_3 (65%), and 6 mL of HCl (37%) in a microwave acid digestion system (MARS 5, CEM Corp., Matthews, NC, USA) for 31 min and diluted to 10 mL with deionized water (digestion conditions for microwave system were applied as 2 min for 250 W, 2 min for 0 W, 6 min for 250 W, 5 min for 400 W, 8 min for 550 W, vent, 8 min). This procedure was preferred because it is more accurate with respect to both time and recovery values. The recovery values were nearly quantitative (>95%) for the above digestion method. A blank digest was carried out in the same way. The concentrations of extracted Pb and Cd were determined by ICP-OES (Perkin Elmer Co., 2100DV).

Lead and cadmium solutions were prepared using $Pb(NO_3)_2$ (Aldrich Chemical Co., <98%) and $Cd(NO_3)_2$ (Kanto Chemical Co., <98%) and the background solution consisted of a mixture of $NaNO_3$ (Kanto Chemical Co., <98%) and MES (2-[N-morpholino]ethanesulfonic acid hydrate, Aldrich Chemical Co., 99.5%) buffer. The effect of carbon dioxide was eliminated by minimizing the head space of the vials. Brunauer–Emmett–Teller (BET) surface area was determined by specific surface area analyzer (Micromeritics, ASAP-2010). Point of zero charge of sediment was determined by potentiometric titration.

2.2. Single- and bi-solute sorption of Pb and Cd onto the sediments

Single-solute sorption experiments were conducted at 25 °C in 50 mL polycarbonate vials (Nalgene Co.). 1.0 g of sediment was transferred into the vial before the addition of heavy metal solutions. To investigate the effect of pH on sorption, pH values of the sediments were adjusted to 2–10 with HNO_3 and NaOH. The vials containing 1.0 g of the sediment each were filled with approximately 50 mL of 2 mM of Pb and Cd solutions at varying pH values. Other than the pH edge experiment, two different pHs (available under natural conditions) were tested because aqueous pH can affect metal sorption. The pH values of the sediments were adjusted to 4.5 or 5.5 by using MES buffer solution (heavy metal free) before all experiments. The vials containing 1.0 g of the sediment each were filled with approximately 50 mL of chemical stock solutions minimizing headspace and then mixed at 10 rpm in a tumbler at 25 °C. The exact amount of the stock solution added was determined gravimetrically. To obtain sorption isotherms, six different initial concentrations of each heavy metal (Pb: 0.24, 1.45, 2.89, 4.34, 5.79 and 7.72 mM; Cd: 0.44, 3.56, 7.12, 10.68, 14.23 and 17.79 mM) were used. The pH values of the heavy metal solutions were also controlled at 4.5 or 5.5 using 0.05 M MES buffer and 0.01 M $NaNO_3$ was added as a background electrolyte. Variation in pH was less than ± 0.05 units. Experiments with this buffer in solutions of

Table 1
The physicochemical characteristics of the coastal sediments used.

		Sediment		
		A	B	C
Location	The north latitude	35°82′12″	34°82′52″	34°87′39″
	The east longitude	126°65′63″	127°40′74″	127°35′74″
pH		8.0	7.9	7.8
Organic carbon (weight %)		0.88	0.76	0.38
CEC (meq/100g)		33.3	35.9	18.0
Surface area (m^2/g)		25.80	36.12	13.30
PZC		9–10	9–10	10–10.5
Indigenous heavy metal content (mg/kg)		Pb = 33.8 Cd = 0.0	Pb = 19.0 Cd = 0.0	Pb = 10.0 Cd = 0.0
Mineral content	Quartz (%)	47	43	52
	Muscovite (%)	36	38	23
	Albite (%)	13	16	22
	Kaolinite (%)	3	3	3

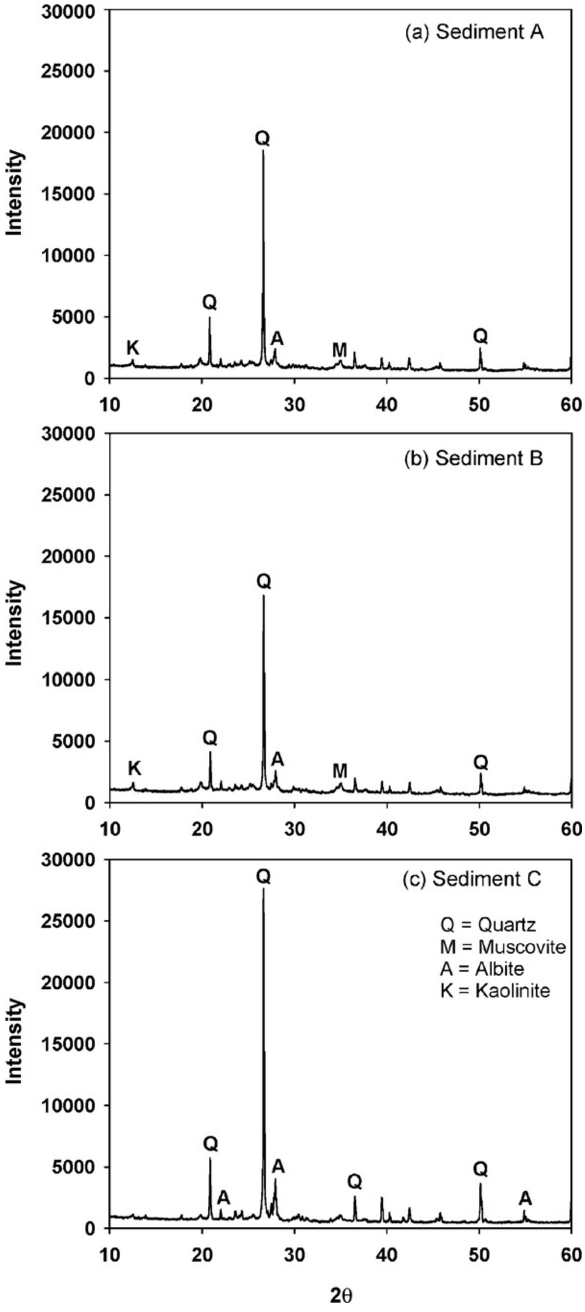

Fig. 1. XRD analyses of the sediments used in this study.

heavy metals confirmed by the results of others [28]; no detectable complexation reactions occur between heavy metals and the MES buffer.

After adding approximately 50 mL of the heavy metal solution into the vial, the mixture was completely mixed in a tumbler at 10 rpm for 24 h. The effect of carbon dioxide was eliminated by minimizing the head space of the vials. Preliminary kinetic experiments showed that sorption equilibrium is reached within 3 h [29]. However, sorption experiments were conducted for 24 h throughout this study to ensure sorption equilibrium [30]. After 24 h of mixing, the vials were collected and centrifuged at 2800 rpm for 20 min. The supernatant was then filtered through 0.2 μm syringe filter (Whatman, cellulose nitrate membrane filter, $\phi = 25$ mm). The aqueous phase equilibrium concentrations of Pb and Cd were determined by ICP-OES (PerkinElmer, 2100DV). The solid phase equilibrium concentrations were calculated by assuming all concentration changes in solution phase result from sorption onto the solid phase. All experiments were run in duplicate. The equilibrium pH was determined by a pH meter (Orion 290A).

Bi-solute competitive systems (Pb^{2+}/Cd^{2+}) were prepared by mixing each metal solution of the same molar concentration (0.24, 1.44, 2.8, 4.34, 5.8 and 7.7 mM) in a 1:1 volume ratio for each solute. Bi-solute competitive sorption experiments were conducted in the same manner as used in the single-solute sorption experiments. The equilibrium concentrations in the mixture were also determined using the ICP-OES.

2.3. Single-solute sorption models

The Freundlich model is often used to describe sorption data:

$$q = K_F C^{N_F} \tag{1}$$

where C (mmol/L) is the aqueous-phase equilibrium concentration, q (mmol/g) is the solid-phase equilibrium concentration, and $K_F[(\text{mmol/g})/(\text{mmol/L})^{N_F}]$ and N_F (−) are the Freundlich sorption coefficient and the Freundlich exponent, respectively.

The Langmuir model for a single-solute sorption is represented as:

$$q = \frac{q_{mL} b_L C}{1 + b_L C} \tag{2}$$

where q_{mL} (mmol/g) and b_L (L/mmol) are the Langmuir parameters that represent the maximum sorption capacity and site energy factor, respectively.

The Dubinin–Radushkevich (D–R) model [31] was applied to distinguish between the physical and chemical sorptions of heavy metals [32].

$$q = q_{mD}\exp(-\beta\varepsilon^2) = q_{mD}\exp\left[-\beta\left(RT\ \ln\left(1+\frac{1}{C}\right)\right)^2\right] \tag{3}$$

where β is a constant related to the mean free energy of sorption per mole of the sorbate ($\mathrm{mol}^2/\mathrm{J}^2$), q_{mD} (mmol/g) is the theoretical saturation capacity and ε is the Polanyi potential, which is equal to $RT\ln(1+1/C)$, where R (J/mol-K) is the gas constant and T (K) is the absolute temperature.

$$\varepsilon = \mathrm{RT}\ \ln\left(1+\frac{1}{C}\right) \tag{4}$$

$$E = \frac{1}{(2\beta)^{1/2}} \tag{5}$$

The constant β gives an idea about the mean free energy E (J/mol) of sorption per molecule of the sorbate when it is transferred to the surface of the solid from infinity in the solution and can be calculated using the relationship [32].

The Sips model is an empirical model for the representing equilibrium sorption data. It is a combination of the Langmuir and Freundlich isotherm type models. The Sips model takes the following form for single solute equilibrium data [10]:

$$q = \frac{q_{mS}(b_S C)^{N_S}}{1+(b_S C)^{N_S}} \tag{6}$$

where q_{mS} (mmol/g), b_S (L/mmol) and N_S (−) are Sips model parameters. If $N_S = 1$, Sips model becomes Langmuir model.

The Redlich–Peterson (R–P) model [33] was defined as:

$$q = \frac{q'_{mR} b_R C}{1+b_R C^{N_R}} \tag{7}$$

where $q'_{mR}[(\mathrm{mmol})^{N_R}/(L^{N_R-1}\,\mathrm{g})]$, b_R $[(\mathrm{L/mmol})^{N_R}]$ and N_R (−) are empirical constants. N_R lies between 0 and 1. The R–P model was slightly modified to calculate the maximum sorption capacity (q_{mR}) of sorbent for comparison:

$$q = \frac{q_{mR} b_R^{1/N_R} C}{1+b_R C^{N_R}} \tag{8}$$

where q_{mR} (mmol/g) is the maximum sorption capacity of sorbent. If $N_R = 1$, the R–P model reduces to Langmuir model. The application of this equation has been successfully applied to several sorption systems [34].

Kargi and Ozmıhcı [35] proposed a generalized model:

$$q = \frac{q_m C^{N_G}}{K_G + C^{N_G}} \tag{9}$$

where q_{mG} (mmol/g) is the maximum sorption capacity of the sorbent, N_G is the cooperative binding constant (−), and K_G (mmol/L) is the saturation constant. If $N_G = 1$, the Kargi–Ozmıhcı model reduces to Langmuir model.

Khan et al. [36] proposed a generalized sorption model:

$$q = \frac{q_{mK} b_K C}{(1+b_K C)^{N_K}} \tag{10}$$

where q_{mK} is the monolayer coverage (mmol/g) and b_K (L/mmol) and N_K (−) are model parameters. If $N_K = 1$, the Khan model reduces to Langmuir model.

The sorption model parameters were determined by using a commercial software package, Table Curve 2D® (Version 5.0, SPSS, Inc.).

2.4. Bi-solute competitive sorption models

The competitive Langmuir model (CLM) [34] was used to analyze bi-solute competitive sorption behaviors. The CLM is an extended form of the Langmuir model which allows predictions of the amount of a solute i sorbed per unit weight of a sorbent, $q_{m,i}$ in the presence of other solutes.

$$q_{m,i} = \frac{q_{mL,i} b_{L,i} C_{m,i}}{1+\sum_{j=1}^{N} b_{L,j} C_{m,j}} \tag{11}$$

where $C_{m,i}$ is the equilibrium concentration of solute i in a mixture consisting of N solutes, and constants $b_{L,i}$ and $q_{mL,i}$ are parameters determined by fitting the Langmuir model to the single-solute sorption data of solute i.

IAST was employed to model competitive bi-solute sorption of Pb and Cd onto sediments. IAST, which was originally proposed by Radke and Prausnitz [37], is of descriptive nature and requires aqueous-phase concentrations to predict sorbed-phase concentrations. To utilize the full predictive power of the IAST, Yen and Singer [38] included the material balance on each solute (i.e., the last equation in Eq. (14)). We followed their modifications of the IAST. IAST is based on the equivalence of spreading pressure in a mixture under equilibrium. The equivalence of spreading pressure in a mixture containing N solutes leads to:

$$\int_0^{q_1^*}\frac{d\log C_1}{d\log q_1}dq_1 = \int_0^{q_2^*}\frac{d\log C_2}{d\log q_2}dq_2 = \cdots = \int_0^{q_N^*}\frac{d\log C_N}{d\log q_N}dq_N \tag{12}$$

or

$$\int_0^{C_1^*}\frac{q_1}{C_1}dC_1 = \int_0^{C_2^*}\frac{q_2}{C_2}dC_2 = \cdots = \int_0^{C_N^*}\frac{q_N}{C_N}dC_N \tag{13}$$

Other equations involved in IAST calculation are:

$$C_{m,i} = z_i C_i^*,\quad \sum_{i=1}^{N} z_i = 1,\quad q_i^* = f(C_i^*),\quad \frac{1}{q_T} = \sum_{i=1}^{N}\frac{z_i}{q_i^*},$$

$$q_{m,i} = z_i q_T = q_{m,i}^0 + \frac{V(C_{m,i}^0 - C_{m,i})}{W} \tag{14}$$

In the above equations, $C_{m,i}$ and $q_{m,i}$ are equilibrium concentrations in the liquid and sorbed phases of a solute i in a mixture, respectively. Superscript 0 in these variables represent initial concentration in N-solute sorption. z_i represents the mole fraction of solute i in the sorbed phase, and C_i^* and q_i^* refer to equilibrium concentrations in the liquid and solid phases of solute i that sorbs singly from solution at the same temperature and spreading pressure as those of the mixture, respectively. The function f in $q_i^* = f(C_i^*)$ denotes a single-solute sorption model for solute i. q_T is the total sorbed concentration of all solutes in the mixture. V and W represent the solution volume and sorbent weight, respectively. There are $5N+1$ equations in total, while $C_{m,i}$, $q_{m,i}$, C_i^*, q_i^*, z_i, and q_T comprise a set of $5N+1$ unknowns. Therefore, we can predict the multisolute sorption data, $q_{m,i}$ vs. $C_{m,i}$, by solving these equations simultaneously. Fortran programs were written to calculate competitive sorption equilibria.

3. Results and discussion

3.1. Sediment characteristics

The result of XRD analysis of the sediment used in this study was shown in Fig. 1 and the physicochemical characteristics were summarized in Table 1. In all sediments, quartz was the dominating (43–52%) mineral followed by muscovite (23–38%), albite (13–22%) and kaolinite (3%). The organic carbon content was in the order of Sediment A (0.88 wt%) > Sediment B (0.76 wt%) > Sediment

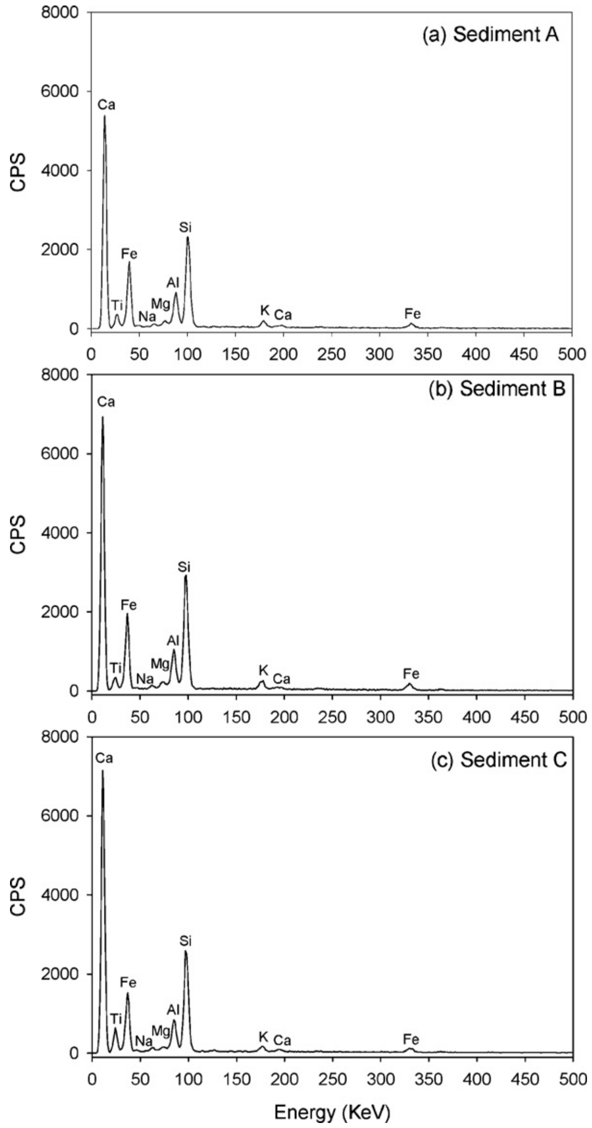

Fig. 2. SEM-EDS analyses of the sediments used in this study.

C (0.38 wt%). The cationic capacity (CEC) was in the order of Sediment B (35.9 meq/100 g) > Sediment A (33.3 meq/100 g) > Sediment C (18.0 meq/100 g). The SEM-EDS analysis (Fig. 2) showed that trace elements in the sediments are Ca, Si, Fe, Al, Mg, Na, K, and Ti. The background metal concentrations in the sediments determined by microwave acid digestion showed that Pb was in trace level (10–40 mg/kg); however, Cd was not detected.

3.2. Effect of pH

Sorptions of Pb and Cd onto sediments as a function of pH were shown in Fig. 3. ($C_0 = 2$ mM). Pb and Cd sorptions increased with increasing pH, with a sharp rise occurring at pH above 6 and 8, respectively. The observed patterns of sorption are typical of cationic sorption. The sorption of metal ions was highly pH dependent, as the charge at the sediment surface and metal ion speciation change with pH. At low pH, the surface groups are protonated producing a positive surface charge, thus cation sorption is unfavorable. At high pH the surface groups are deprotonated and therefore become more negatively charged favoring cation sorption. This is coupled with proton release making sorption more favorable at high pH values [39]. The solution speciation of Pb and Cd were calculated using MINEQL+ (Version 4.5) and shown in Fig. 4. Pb^{2+} is the dominant Pb species in solution at pH below 5; at pH values above 6, $Pb(OH)_2$ precipitates are formed. Cd^{2+} is the dominant Cd species in solution at pH below 8; at pH values above 8, $Cd(OH)_2$ precipitates are dominant.

The pH of aqueous solutions of Pb and Cd were adjusted and filtered through a 0.45 μm membrane filter. As depicted in Fig. 3, the amount of metal precipitates formed (the right y axis) determined by membrane filtration increased as pH increased with a sharp rise at pH > 5 for Pb and at pH > 8 for Cd, respectively. Nearly 45% of Pb sorption at pH > 8 and 98% of Cd sorption at pH > 9, respectively, was attributed to precipitate formation. These patterns are matching with sorption supporting that precipitate formation is one of the major metal sorption mechanisms. The pH_{50} value where 50% of initially spiked heavy metal is sorbed was in the order of Sediment C (= 6.2) > Sediment B (= 3.5) > Sediment A (= 2.9) for Pb and in the order of Sediment C (= 8.1) > Sediment A (= 6.3) > Sediment B (= 5.6) for Cd, respectively.

3.3. Single-solute sorption

Single-solute sorptions of Pb (Fig. 5) and Cd (Fig. 6) onto sediments were conducted at pHs 4.5 and 5.5. Both Pb and Cd exhibited isotherms of type L [40], which were very close to irreversible sorption. Such isotherms are characteristic of strong adsorbate–adsorbent interactions. Comparison of Figs. 5 and 6 showed that the sorption affinity, as represented by Freundlich sorption coefficient (K_F) and Langmuir sorption capacity (q_{mL}), of Pb was higher than that of Cd except Sediment B at pH 4.5. The sorption affinity of Pb onto the sediments was in the order of Sediment B ≈ Sediment A > Sediment C (Fig. 5). The sorption affinity

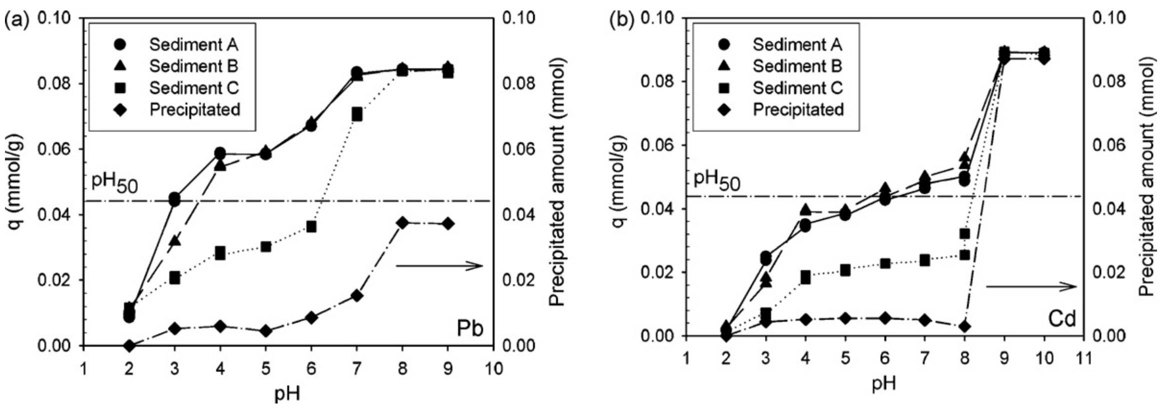

Fig. 3. Effect of pH on the adsorption of Pb and Cd onto sediments.

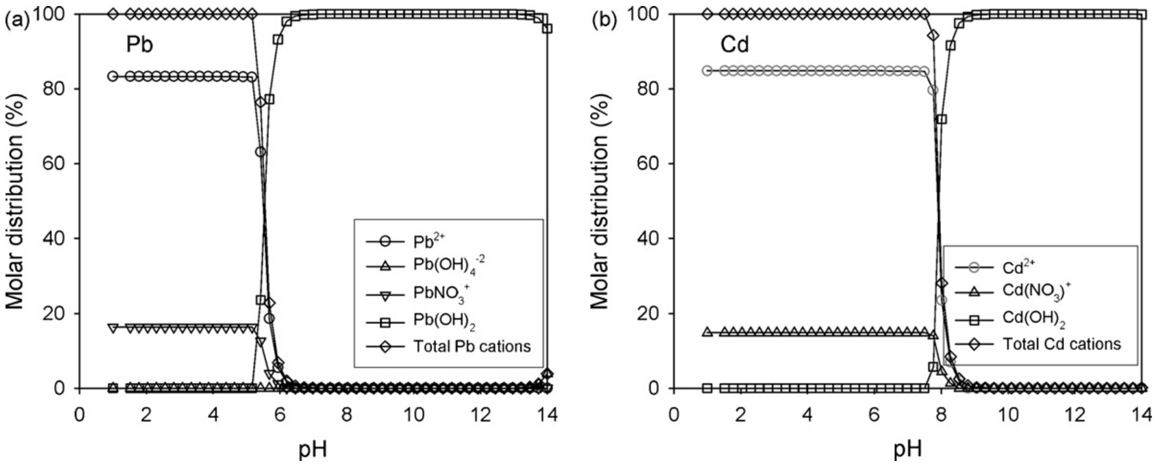

Fig. 4. Distribution of total Pb and Cd concentrations as a function of pH predicted using MINEQL+ 4.5 software.

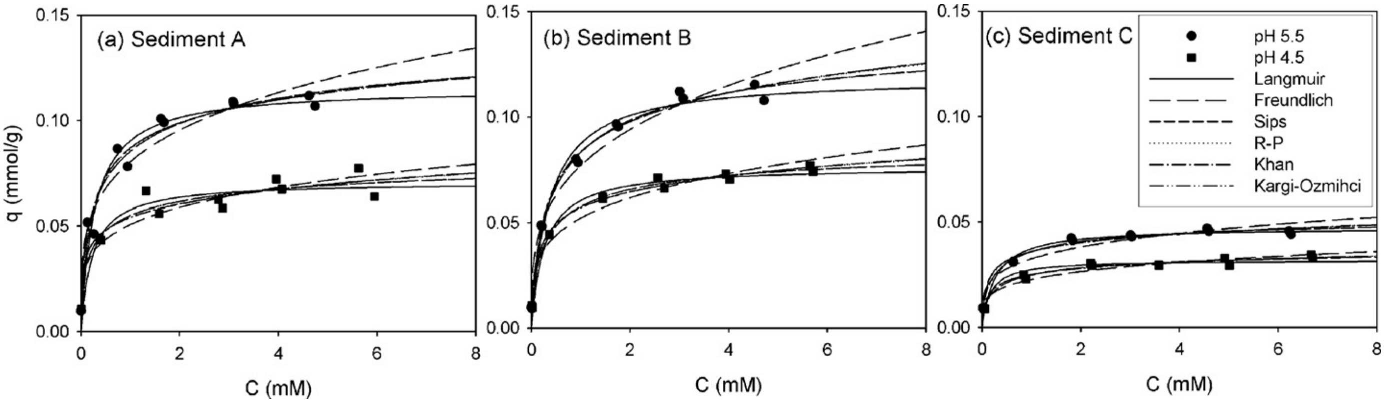

Fig. 5. Single-solute adsorption of Pb onto sediments. Lines represent adsorption models.

of Cd onto sediments was in the order of Sediment B > Sediment A > Sediment C (Fig. 6). For both heavy metals, sorption affinity at pH 5.5 was higher than that of pH 4.5 except Sediment B and C for Cd where the difference in Cd sorption between pH 4.5 and 5.5 was not noticeable. The difference in sorption between pH 4.5 and 5.5 is attributed to: (i) the role of H^+ ions in competition with metal cations for sorption sites decreases with increasing pH and (ii) some portion of metal ions are precipitated by forming metal hydroxides with increasing pH. In this study, Pb^{2+} and Cd^{2+} ions were the dominant (>80%) at pH 4.5 (see Fig. 4). However, about 50% of Pb^{2+} ion concentration decreased and precipitated as $Pb(OH)_2$ at pH 5.5, whereas Cd^{2+} was still dominant. In other words, Pb^{2+} ion can not only sorbed onto sediments but also precipitated as metal hydroxides at pH 5.5, whereas Pb^{2+} ions are only sorbed, but not precipitated at pH 4.5. Therefore, the difference in Pb sorption between pH 4.5 and 5.5 is attributed to both competitive sorption between metal cations and H^+ ions and precipitate formation. In contrast, difference in Cd sorption between pH 4.5 and 5.5 was not noticeable in Sediment B and C (except Sediment A) because Cd^{2+} was sorbed competitively with H^+ ions for sorption sites but not precipitated in these pH ranges (see Section 3.2 and Fig. 4). The order of increase in sorption affinity was consistent with CEC and BET surface area but not with organic carbon content (see Table 1).

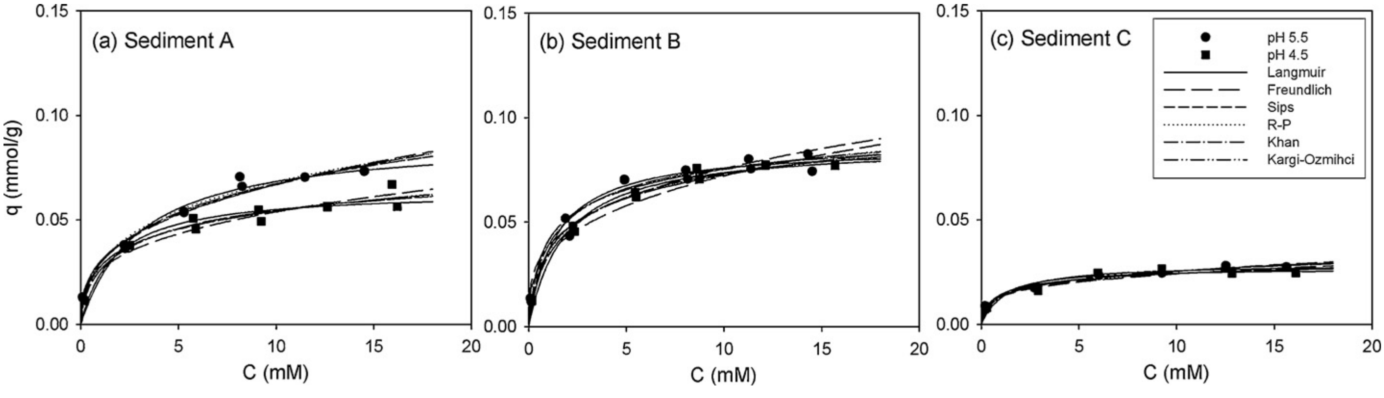

Fig. 6. Single-solute adsorption of Cd onto sediments. Lines represent adsorption models.

Several sorption models: Freundlich, Langmuir, Dubinin–Radushkevich, Sips, Redlich–Peterson, Kargi–Ozmıhcı and Khan models were fitted to the sorption data by using the nonlinear regression method. The Freundlich model parameters were listed in Table 2. The Freundlich model fitted the experimental data well ($0.87 < R^2 < 0.98$). The Freundlich sorption constant, K_F, indicates the sorption capacity of the sorbent. The K_F value was in the order of Sediment B > Sediment A > Sediment C except Pb at pH 5.5. The K_F values of Pb were higher than those of Cd and the values at pH 5.5 were consistently higher than those at pH 4.5. The Freundlich exponent, N_F, is a measure of the deviation from linearity of the sorption. When N_F is equal to unity, the sorption is linear. If $N_F < 1$ or $N_F > 1$, the sorption is non-linear. Especially, N_F value in the range of $0.1 < N_F < 1$ indicates that the sorption is favorable [41,42]. In this study, the N_F values for sorptions of Pb and Cd onto sediments were in the range of 0.22–0.36, representing that Pb and Cd sorption was nonlinear and favorable.

The Langmuir model parameters were listed in Table 3. The Langmuir model fitted the experimental data well ($0.88 < R^2 < 0.99$). The maximum sorption capacity (q_{mL}) of Pb and Cd was in the order of Sediment B > Sediment A > Sediment C. The q_{mL} values of Pb were higher than Cd and the values at pH 5.5 were consistently higher than those at pH 4.5 except Cd sorption onto Sediment B. The essential characteristic of Langmuir isotherm can be expressed in terms of a dimensionless constant, separation factor R_L (−), that describe the type of isotherm [43].

$$R_L = \frac{1}{1 + b_L C_0} \tag{15}$$

where b_L is the Langmuir constant and C_0 is the initial concentration of metal solution. The values of R_L indicates the type of isotherm to be unfavorable ($R_L > 1$), linear ($R_L = 1$), favorable ($0 < R_L < 1$) or irreversible ($R_L = 0$). The values of R_L calculated at the maximum initial concentrations ($C_{0,\max} = 7.72$ mM for Pb and 17.79 mM for Cd) were between 0.02 and 0.15 (Table 3), indicating that sorptions of Pb and Cd onto the sediments are favorable.

The 2-parameter D–R model was fitted to the single-solute sorption data (Table 4). The D–R model did not fit the data well ($0.78 < R^2 < 0.95$). The q_{mD} value of the D–R model increased in the order of Sediment B > Sediment A > Sediment C for both heavy metals. The q_{mD} values at pH 5.5 were higher than those at pH 4.5. As represented in Table 3, the q_{mD} values of D–R model were nearly same as the q_{mL} values of the Langmuir model. However, it is difficult to explain the similarity between the q_{mD} and q_{mL} values because both models have different sorption mechanisms. D–R model is based on the interaction between sorbent and the volume of sorbate residing within the uniform micropores [44], whereas the Langmuir model is based on the interaction between sorbate and surface area of sorbent. The relationship between the q_{mD} and q_{mL} were not consistent in previous studies. Apiratikul and Pavasant [45] reported that the q_{mD} values were similar with q_{mL} values. However, in other studies [46–48], the q_{mD} values were widely different from the q_{mL} values. The value of mean free energy E in D–R model gives information whether sorption mechanism is ion-exchange or physical sorption. If the magnitude of E is between 8 and 16 kJ/mol, the sorption process follows ion-exchange, while for the values of $E < 8$ kJ/mol, the sorption process is of a physical nature. For the values of $E > 16$ kJ/mol, the sorption occurs via chemical sorption [32]. In this study, the calculated E values were less than 8 kJ/mol indicating that sorption of Pb and Cd onto the sediments occurs via physisorption due to weak van der Waals forces [32].

The Sips, R–P, Kargi–Ozmıhcı and Khan model parameters were listed in Tables 5–8, respectively. In terms of R^2 values, the 3-parameter Sips ($R^2 > 0.92$), R–P ($R^2 > 0.90$), Kargi–Ozmıhcı

Table 2
Freundlich model parameters for single-solute adsorption of Pb and Cd.

Solute	Sediment	pH	K_F [(mmol/g)/(mmol/L)^{N_F}]	N_F (−)	R^2	SSE
Pb	A	4.5	0.0507 ± 0.0023	0.2151 ± 0.0310	0.9210	0.0004
	B		0.0521 ± 0.0019	0.2452 ± 0.0265	0.9511	0.0003
	C		0.0228 ± 0.0009	0.2203 ± 0.0253	0.9353	0.0001
	A	5.5	0.0805 ± 0.0028	0.2468 ± 0.0276	0.9551	0.0007
	B		0.0770 ± 0.0025	0.2899 ± 0.0269	0.9665	0.0005
	C		0.0326 ± 0.0014	0.2273 ± 0.0285	0.9321	0.0001
Cd	A	4.5	0.0261 ± 0.0020	0.3149 ± 0.0327	0.9521	0.0002
	B		0.0345 ± 0.0025	0.3202 ± 0.0310	0.9603	0.0003
	C		0.0135 ± 0.0013	0.2527 ± 0.0407	0.8726	0.0001
	A	5.5	0.0294 ± 0.0017	0.3577 ± 0.0256	0.9795	0.0001
	B		0.0383 ± 0.0032	0.2954 ± 0.0379	0.9332	0.0004
	C		0.0132 ± 0.0006	0.2831 ± 0.0190	0.9769	0.0000

Table 3
Langmuir model parameters for single-solute adsorption of Pb and Cd.

Solute	Sediment	pH	q_{mL} (mmol/g)	b_L (L/mmol)	R^2	SSE	R_L[a]
Pb	A	4.5	0.0709 ± 0.0034	4.3665 ± 1.4878	0.9207	0.0004	0.0288
	B		0.0764 ± 0.0020	3.7876 ± 0.6267	0.9781	0.0001	0.0347
	C		0.0319 ± 0.0010	6.0558 ± 1.6533	0.9387	0.0001	0.0331
	A	5.5	0.1154 ± 0.0048	3.6011 ± 0.8020	0.9303	0.0006	0.0448
	B		0.1190 ± 0.0038	2.7627 ± 0.4218	0.9807	0.0003	0.0209
	C		0.0475 ± 0.0016	3.6817 ± 0.8932	0.9624	0.0001	0.0340
Cd	A	4.5	0.0643 ± 0.0033	0.5863 ± 0.1488	0.9483	0.0002	0.0875
	B		0.0874 ± 0.0028	0.5365 ± 0.0801	0.9821	0.0001	0.1472
	C		0.0269 ± 0.0014	1.0106 ± 0.3308	0.8865	0.0001	0.0948
	A	5.5	0.0894 ± 0.0058	0.3256 ± 0.0731	0.9580	0.0002	0.0727
	B		0.0865 ± 0.0037	0.7173 ± 0.1568	0.9644	0.0002	0.0527
	C		0.0289 ± 0.0015	0.7659 ± 0.2223	0.9207	0.0000	0.0684

[a] Calculated at $C_0 = 7.72$ mM for Pb and at $C_0 = 17.79$ mM for Cd, respectively.

Table 4
Dubinin–Radushkevich model parameters for single-solute adsorption of Pb and Cd.

Solute	Sediment	pH	q_{mD} (mmol/g)	β (mol^2/J^2, × 10^{-8})	R^2	SSE	E (kJ/mol)
Pb	A	4.5	0.0675 ± 0.0028	4.3494 ± 1.2838	0.9043	0.0005	3.39
	B		0.0717 ± 0.0021	4.4251 ± 0.8573	0.9533	0.0003	3.36
	C		0.0304 ± 0.0009	2.1974 ± 0.3918	0.9136	0.0001	4.77
	A	5.5	0.1057 ± 0.0040	3.8652 ± 0.7604	0.9400	0.0010	3.60
	B		0.1064 ± 0.0035	4.6657 ± 0.7567	0.9551	0.0007	3.27
	C		0.0431 ± 0.0014	2.2135 ± 0.5241	0.9219	0.0002	4.75
Cd	A	4.5	0.0574 ± 0.0028	66.718 ± 21.229	0.8713	0.0004	0.866
	B		0.0769 ± 0.0027	65.922 ± 14.049	0.9347	0.0004	0.871
	C		0.0237 ± 0.0011	7.9245 ± 2.1873	0.7832	0.0001	2.51
	A	5.5	0.0719 ± 0.0031	88.176 ± 18.652	0.9147	0.0005	0.753
	B		0.0782 ± 0.0028	49.092 ± 11.161	0.9307	0.0005	1.01
	C		0.0245 ± 0.0011	6.9836 ± 1.9936	0.7909	0.0001	2.68

Table 5
Sips model parameters for single-solute adsorption of Pb and Cd.

Solute	Sediment	pH	q_{mS} (mmol/g)	b_S (L/mmol)	N_S (−)	R^2	SSE
Pb	A	4.5	0.0887 ± 0.0170	2.7289 ± 2.6888	0.4859 ± 0.1309	0.9515	0.0003
	B		0.0885 ± 0.0051	2.6852 ± 0.6475	0.6303 ± 0.0650	0.9926	0.0000
	C		0.0390 ± 0.0038	2.6974 ± 1.2437	0.5769 ± 0.0960	0.9761	0.0000
	A	5.5	0.1544 ± 0.0328	1.5171 ± 1.4178	0.5136 ± 0.1298	0.9749	0.0004
	B		0.1453 ± 0.0154	1.5647 ± 0.6008	0.6555 ± 0.0955	0.9902	0.0002
	C		0.0542 ± 0.0034	2.9915 ± 0.8639	0.6201 ± 0.0713	0.9878	0.0000
Cd	A	4.5	0.0860 ± 0.0190	0.2487 ± 0.2050	0.6055 ± 0.1330	0.9700	0.0001
	B		0.1028 ± 0.0085	0.3611 ± 0.1015	0.7072 ± 0.0764	0.9919	0.0001
	C		0.0323 ± 0.0070	0.5899 ± 0.5039	0.6434 ± 0.2123	0.9153	0.0000
	A	5.5	0.2021 ± 0.1289	0.0233 ± 0.0541	0.4763 ± 0.1033	0.9825	0.0001
	B		0.0981 ± 0.0120	0.5515 ± 0.2409	0.7178 ± 0.1374	0.9731	0.0002
	C		0.0525 ± 0.0163	0.0878 ± 0.1211	0.4490 ± 0.0835	0.9844	0.0000

Table 6
Redlich–Peterson model parameters for single-solute adsorption of Pb and Cd.

Solute	Sediment	pH	q_{mR} (mmol/g)	b_R [(L/mmol)^{N_R}]	N_R (−)	R^2	SSE
Pb	A	4.5	0.0272 ± 0.0091	55.447 ± 39.711	0.8503 ± 0.0379	0.9494	0.0003
	B		0.0420 ± 0.0071	12.609 ± 4.2682	0.8685 ± 0.0257	0.9899	0.0001
	C		0.0269 ± 0.0013	13.850 ± 4.4749	0.8836 ± 0.0301	0.9762	0.0000
	A	5.5	0.0760 ± 0.0296	7.6008 ± 5.3442	0.8886 ± 0.0768	0.9655	0.0005
	B		0.0742 ± 0.0187	5.9278 ± 2.4034	0.8668 ± 0.0503	0.9880	0.0002
	C		0.0270 ± 0.0046	14.630 ± 5.0561	0.8830 ± 0.0282	0.9804	0.0000
Cd	A	4.5	0.0279 ± 0.0109	2.9593 ± 1.8496	0.8036 ± 0.0568	0.9713	0.0001
	B		0.0479 ± 0.0110	1.8870 ± 0.7630	0.8390 ± 0.0426	0.9888	0.0001
	C		0.0166 ± 0.0071	2.7288 ± 2.1159	0.8754 ± 0.0834	0.9044	0.0000
	A	5.5	0.0069 ± 0.0093	19.609 ± 37.271	0.6636 ± 0.0469	0.9802	0.0001
	B		0.0520 ± 0.0176	2.2171 ± 1.4322	0.8660 ± 0.0659	0.9682	0.0002
	C		0.0082 ± 0.0033	8.0823 ± 5.4788	0.7700 ± 0.0363	0.9824	0.0000

Table 7
Kargi–Ozmıhci model parameters for single-solute adsorption of Pb and Cd.

Solute	Sediment	pH	q_{mG} (mmol/g)	K_G (mmol/L)	N_G (−)	R^2	SSE
Pb	A	4.5	0.0887 ± 0.0170	0.6140 ± 0.3619	0.4859 ± 0.1309	0.9515	0.0003
	B		0.0885 ± 0.0051	0.5365 ± 0.1098	0.6303 ± 0.0650	0.9926	0.0000
	C		0.0390 ± 0.0038	0.5642 ± 0.1962	0.5769 ± 0.0960	0.9761	0.0000
	A	5.5	0.1544 ± 0.0328	0.8073 ± 0.4270	0.5136 ± 0.1298	0.9749	0.0004
	B		0.1453 ± 0.0154	0.7457 ± 0.2161	0.6555 ± 0.0955	0.9902	0.0002
	C		0.0542 ± 0.0034	0.5069 ± 0.1218	0.6201 ± 0.0713	0.9878	0.0000
Cd	A	4.5	0.0860 ± 0.0190	2.3225 ± 0.7950	0.6055 ± 0.1330	0.9700	0.0001
	B		0.1028 ± 0.0085	2.0551 ± 0.2890	0.7072 ± 0.0764	0.9919	0.0001
	C		0.0323 ± 0.0070	1.4044 ± 0.6428	0.6434 ± 0.2123	0.9153	0.0000
	A	5.5	0.2021 ± 0.1289	5.9869 ± 4.4178	0.4763 ± 0.1033	0.9825	0.0001
	B		0.0981 ± 0.0120	1.5330 ± 0.3927	0.7178 ± 0.1374	0.9731	0.0002
	C		0.0525 ± 0.0163	2.9805 ± 1.2752	0.4490 ± 0.0835	0.9844	0.0000

Table 8
Khan model parameters for single-solute adsorption of Pb and Cd.

Solute	Sediment	pH	q_{mK} (mmol/g)	b_K(L/mmol)	N_K (−)	R^2	SSE
Pb	A	4.5	0.0267 ± 0.0182	99.500 ± 83.13	0.8450 ± 0.0374	0.9489	0.0003
	B		0.0397 ± 0.0067	17.290 ± 7.52	0.8560 ± 0.0265	0.9891	0.0001
	C		0.0184 ± 0.0031	17.950 ± 6.85	0.8752 ± 0.0303	0.9760	0.0000
	A	5.5	0.0753 ± 0.0280	8.276 ± 6.566	0.8845 ± 0.0803	0.9646	0.0006
	B		0.0696 ± 0.0175	7.185 ± 3.589	0.8504 ± 0.0526	0.9876	0.0002
	C		0.0256 ± 0.0044	20.160 ± 8.539	0.8728 ± 0.0292	0.9790	0.0000
Cd	A	4.5	0.0252 ± 0.0085	3.570 ± 2.444	0.7806 ± 0.0521	0.9715	0.0000
	B		0.0416 ± 0.0097	2.235 ± 1.062	0.8090 ± 0.0427	0.9877	0.0000
	C		0.0156 ± 0.0065	3.001 ± 2.515	0.8620 ± 0.0847	0.9025	0.0000
	A	5.5	0.0082 ± 0.0085	43.710 ± 108.15	0.6541 ± 0.0381	0.9799	0.0001
	B		0.0468 ± 0.0163	2.565 ± 1.9264	0.8430 ± 0.0676	0.9669	0.0002
	C		0.0083 ± 0.0027	10.583 ± 7.9728	0.7583 ± 0.0327	0.9816	0.0000

($R^2 > 0.92$) and Khan ($R^2 > 0.97$) models were better than the 2-parameter Freundlich ($R^2 > 0.87$), Langmuir ($R^2 > 0.88$), and D–R ($R^2 > 0.78$) models as expected from the number of parameters involved in the models.

As listed in Table 5, the q_{mS} values of Sips model increased in the order of Sediment A > Sediment B > Sediment C except Cd sorption at pH 4.5. The q_{mS} value was not correlated with CEC and BET surface area of the sediments, indicating that Sips model cannot explain sorption behaviors of Pb and Cd well. The q_{mS} values at pH 5.5 were higher than those at pH 4.5 except Cd sorption onto Sediment B.

The Redlich–Peterson model [33] parameters were shown in Table 6. The q_{mR} values of the R–P model were in the order of Sediment B > Sediment A > Sediment C. The q_{mR} values were dependent on CEC and BET surface area of the sediment except Pb sorption at pH 5.5 and Cd sorption at pH 5.5 and also showed similar trend with the q_{mL} of Langmuir, the q_{mD} of D–R models, the q_{mK} of Khan, but different trend from the q_{mS} of Sips model and q_{mG} of Kargi-Ozmıhcı model. The q_{mR} values at pH 5.5 were also higher than those at pH 4.5 except Cd sorption onto Sediment A and C.

The Kargi–Ozmıhcı model [35] parameters for single-solute sorption were listed in Table 7. The R^2 values of the Kargi–Ozmıhcı model (0.92–0.99) were nearly the same goodness-of-fit as the Sips, R–P and Khan models (see below). In Table 7, the q_{mG} value of the Kargi–Ozmıhcı model increased in the order of Sediment A > Sediment B > Sediment C except Cd sorption at pH 4.5. The q_{mG} values at pH 5.5 were higher than those at pH 4.5 except Cd sorption onto Sediment B. The increase in q_{mG} value was consistent with the q_{mS} value of Sips model.

The Khan model [36] parameters were listed in Table 8. The R^2 values of the Khan model ($0.97 < R^2 < 0.99$) showed nearly the same goodness-of-fit as the other 3-parameter Sips, R–P and the Kargi–Ozmıhci models. As listed in Table 8, the q_{mK} values of the Khan model increased in the order of Sediment B > Sediment A > Sediment C consistent with CEC and BET surface area of the sediments, except Pb sorption at pH 5.5. The increase in q_{mK} value was consistent with the increase in the q_{mL} value of the Langmuir, the q_{mD} value of D–R, and q_{mR} value of R–P models, but not with the q_{mS} value of Sips and q_{mG} value of Kargi–Ozmıhci models.

3.4. Bi-solute competitive sorption

Bi-solute competitive sorption experiments were performed. As expected, when two solutes compete for sorption in the bi-solute system, the sorbed amount of each solute was less than that in a single-solute system. The solute with a lower sorption affinity (i.e., Cd) in single-solute system showed a higher reduction of sorbed amount in bi-solute system.

The bi-solute competitive sorptions of Pb and Cd onto sediments were analyzed by the Langmuir model (Table 9). The R^2 values (<0.97) indicate that the Langmuir model was not fitting the bi-solute competitive sorptions well. In comparison of single-solute sorptions (Table 3), the q_{mL} values for bi-solute sorptions were reduced due to competition at both pH values. In both single- and bi-solute sorptions, the Langmuir parameters, q_{mL} and b_L, were not correlated. All sediments exhibited similar sorption patterns; the q_{mL} values of Pb were higher than those of Cd regardless of whether the metals were applied in single- or bi-solute competitive sorptions with the only exception of single-solute sorption in sediment B at pH 4.5.

In Table 10, the estimated maximum sorption capacity values of bi-solute competitive sorption (q^*_{mL}) were compared with those of single-solute sorption (q_{mL}). In all sediments, the $q_{mL,Pb}/q_{mL,Cd}$

Table 9
Langmuir model parameters for bi-solute competitive adsorption of Pb and Cd.

Sediment	pH	Solute	q^*_{mL} (mmol/g)	b^*_L (L/mmol)	R^2	SSE
A	4.5	Pb/Cd	0.071 ± 0.002	2.712 ± 0.512	0.972	0.0002
		Cd/Pb	0.032 ± 0.003	0.809 ± 0.238	0.919	0.0001
B		Pb/Cd	0.075 ± 0.003	2.521 ± 0.525	0.966	0.0002
		Cd/Pb	0.038 ± 0.003	0.873 ± 0.272	0.911	0.0001
C		Pb/Cd	0.041 ± 0.002	1.622 ± 0.449	0.941	0.0001
		Cd/Pb	0.032 ± 0.005	0.360 ± 0.140	0.878	0.0001
A	5.5	Pb/Cd	0.099 ± 0.005	1.500 ± 0.320	0.962	0.0004
		Cd/Pb	0.020 ± 0.002	1.520 ± 0.780	0.735	0.0001
B		Pb/Cd	0.089 ± 0.003	2.681 ± 0.525	0.969	0.0003
		Cd/Pb	0.022 ± 0.002	4.609 ± 2.690	0.716	0.0001
C		Pb/Cd	0.046 ± 0.003	1.307 ± 0.374	0.929	0.0001
		Cd/Pb	0.024 ± 0.006	0.306 ± 0.170	0.728	0.0001

q^*_{mL} and b^*_{mL} indicates q_{mL} value and b_{mL} value for bi-solute competitive adsorption, respectively.

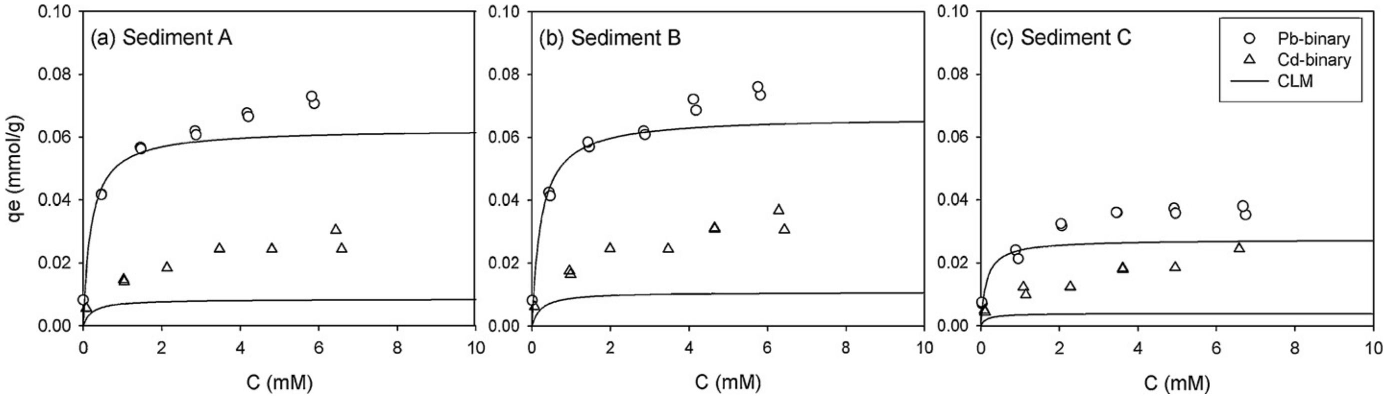

Fig. 7. Bi-solute competitive adsorption of Pb and Cd at pH 4.5. Lines represent CLM predictions.

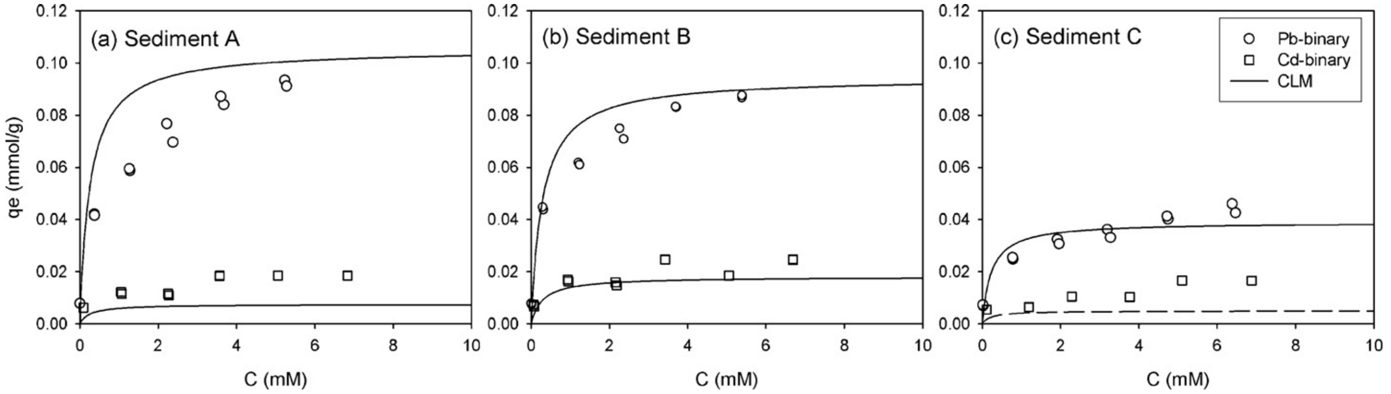

Fig. 8. Bi-solute competitive adsorption of Pb and Cd at pH 5.5. Lines represent CLM predictions.

ratios (0.87–1.19 at pH 4.5 and 1.30–1.62 at pH 5.5, respectively) were lower than the $q^*_{mL,Pb}/q^*_{mL,Cd}$ ratios (1.28–2.22 at pH 4.5 and 1.92–4.95 at pH 5.5, respectively). This confirms the higher sorption affinity of Pb than Cd for sediments. This was generally found in both pure soil components and heterogeneous soils [2,49–51]. The $q_{mL,i}/q^*_{mL,i}$ ratios were generally greater than unity (except for Cd in Sediment C at pH 4.5) suggesting that the simultaneous presence of both metals reduced sorption due to competition for sorption sites in the sediments. In addition, it was generally true that $q_{mL,Cd}/q^*_{mL,Cd} > q_{mL,Pb}/q^*_{mL,Pb}$ indicating that Cd sorption was more affected by the simultaneous presence of a competing metal than Pb sorption. This tendency of higher sorption of Pb on different surfaces was reported in the presence of Cd [1,2,51], Cu [52] and other metals in multi-metal solutions [53,54]. Saha et al. [54] found no competition between Pb and other metals at low concentrations. In Sediment C, however, $q_{mL,Cd}/q^*_{mL,Cd}$ and $q_{mL,Pb}/q^*_{mL,Pb}$ ratios were similar and smaller than unity at pH 4.5, but slightly above unity at pH 5.5.

Table 10
Comparison of q_{mL} and b_{L} values of single-solute and bi-solute competitive adsorption of Pb and Cd.

pH	Sediment	$q_{mL,Pb}/q_{mL,Cd}$	$q^*_{mL,Pb}/q^*_{mL,Cd}$	$q_{mL,Pb}/q^*_{mL,Pb}$	$q_{mL,Cd}/q^*_{mL,Cd}$
4.5	A	1.131	2.294	0.975	2.029
	B	0.874	2.011	1.009	2.322
	C	1.190	1.283	0.781	0.842
5.5	A	1.292	5.059	1.161	4.547
	B	1.376	4.060	1.340	3.954
	C	1.641	1.914	1.021	1.191

pH	Sediment	$b_{L,Pb}/b_{L,Cd}$	$b^*_{L,Pb}/b^*_{L,Cd}$	$b_{L,Pb}/b^*_{L,Pb}$	$b_{L,Cd}/b^*_{L,Cd}$
4.5	A	7.448	3.352	1.610	0.725
	B	7.060	2.888	1.502	0.615
	C	5.992	4.504	3.733	2.801
5.5	A	11.06	0.987	2.401	0.214
	B	3.852	0.582	1.031	0.156
	C	4.807	4.268	2.818	2.502

$q_{mL,Pb}$ and $q_{mL,Cd}$ indicate q_{mL} values for single-solute adsorption and $q^*_{mL,Pb}$ and $q^*_{mL,Cd}$ indicates q_{mL} values for bi-solute competitive adsorption, respectively. $b_{mL,Pb}$ and $b_{mL,Cd}$ indicate b_{mL} values for single-solute adsorption and $b^*_{mL,Pb}$ and $b^*_{mL,Cd}$ indicates b_{mL} values for bi-solute competitive adsorption, respectively.

The binding energy coefficient (b_{Pb} and b_{Cd} for single-solute sorption and b^*_{Pb} and b^*_{Cd} for bi-solute competitive sorption, respectively) varied with sediment type and metal solution, although all sediments showed greater affinity for Pb than for Cd as $b_{Pb} > b_{Cd}$ and $b^*_{Pb} > b^*_{Cd}$ except Sediment A and B at pH 5.5 (see Tables 3 and 10). Adhikari and Singh [50] found similar results for single metal solutions. The results of Rodríguez-Maroto [1] for both single and binary solutions also agreed with the generally accepted metal affinity series for soils and soil components [49]. However, in contrast to

Table 11
R^2 and SSE values for bi-solute competitive adsorption predictions from competitive Langmuir model (CLM).

pH	Sediment	R^2 (Pb/Cd)	SSE (Pb/Cd)
4.5	A	0.9872/0.5663	0.0002/0.0011
	B	0.9887/0.5893	0.0002/0.0015
	C	0.9384/0.3637	0.0003/0.0010
5.5	A	0.9229/0.6496	0.0020/0.0005
	B	0.9831/0.9309	0.0004/0.0001
	C	0.9813/0.5666	0.0001/0.0004

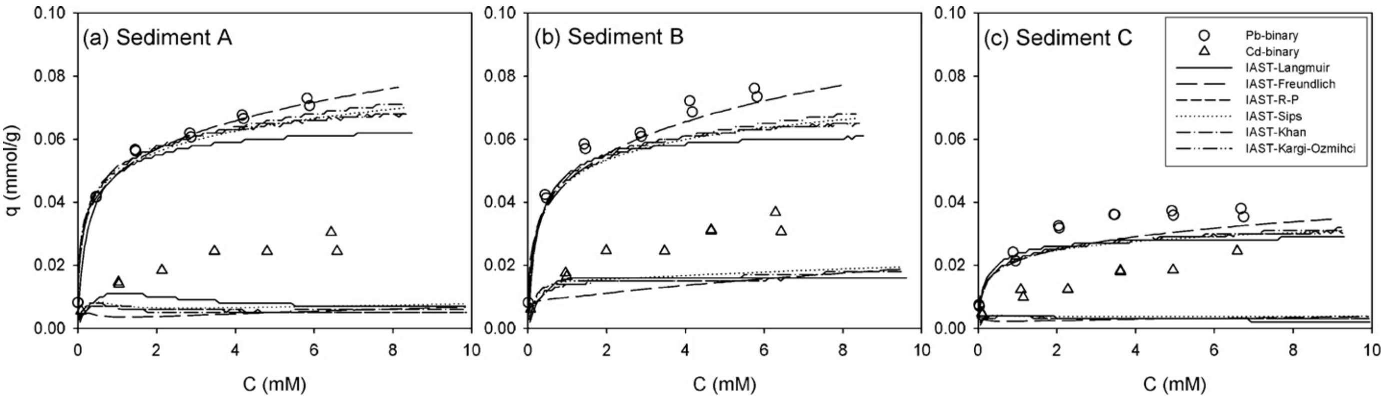

Fig. 9. Bi-solute competitive adsorption of Pb and Cd at pH 4.5. Lines represent IAST predictions coupled to the single-solute adsorption models.

those researchers, our study found $b_i > b_i^*$ in all sediments except Cd in sediment A and B at both pHs at 4.5 and 5.5 as a result of the simultaneous presence of both metals, which is in agreement with Mesquita and Vieira e Silva [55] for competitive sorption of Cu and Zn where $b_i < b_i^*$ was found for both Cu and Zn in three of four soil samples. This indicates that competition for sorption sites promotes the retention of Cd on more specific sorption sites, except for sediment C where b_L^* values of both metals decreased.

While binding strength, or affinity constant (b), estimates made from sorption isotherms should only be considered qualitatively [56], they have been related to the free energy change of sorption of different species [57]. Higher b values have been related to specifically sorbed metals at high energy surfaces with low dissociation constants. Alternatively, lower b values appear to be related to sorption at low energy surfaces with high dissociation constants [2,50]. The bi-solute isotherm b_i^* values of Pb were less than the single-solute isotherm b_i values in all sediments indicating that competition for sorption sites decreases the retention of Pb on more specific sorption positions. As a result, maximum sorption coefficient ($q_{mL,i}$) decreases and thus the metals are held less strongly. The irregular sorptive behavior of Sediment C in this regard could be explained by the high metal load relative to its low sorption capacity as indicated by the CEC and BET surface area [2]. Thus, the estimated b_i^* values of both Pb and Cd decreased in Sediment C as a consequence of the increased sorption levels or sorption capacity values ($q_{mL,i}^*$). The $q_{mL,i}^*$ value was in the order of Sediment B > Sediment A > Sediment C at both pHs except Cd at pH 5.5 and the order of decrease in $q_{mL,i}^*$ was consistent with CEC and BET surface area (see Table 1). Our results demonstrate that the bi-solute competitive sorption of Pb and Cd depends on sediment properties such as the clay mineralogy, CEC and BET surface area in agreement with the previous reports [14,50].

The CLM predictions for competitive sorption of Pb and Cd at pHs 4.5 and 5.5 were shown in Figs. 7 and 8, respectively, together with the experimental data for comparison. The predictions of CLM were successful in Pb sorption but not in Cd sorption in terms of R^2 values (Table 11).

IAST predictions for the competitive bi-solute sorption at pHs 4.5 and 5.5 were shown in Figs. 9 and 10, respectively. Bi-solute predictive IAST was coupled with the single-solute sorption models: Freundlich, Langmuir, Sips, Redlich–Peterson, Kargi–Ozmıhcı and Khan models, the parameters of which were previously determined from the nonlinear curve-fitting to the single-solute sorption data (see Tables 2–8). To compare predictions with the experimental data, R^2 and the sum of squared errors (SSE) from the following equation were calculated and listed in Table 12.

$$R^2 = \frac{\sum q_i^2 - SSE}{\sum q_i^2} \tag{16}$$

where

$$SSE = \sum (q_i - \tilde{q}_i)^2 \tag{17}$$

In the above equation, $\tilde{q}_i$ denotes the uptake of a solute predicted by IAST. As indicated by the R^2 and SSE values in Table 12, the IAST prediction varied with single-solute sorption model, sediment type, pH and metal solution. The IAST predictions for the most of the competitive sorptions were in good agreement with data except a

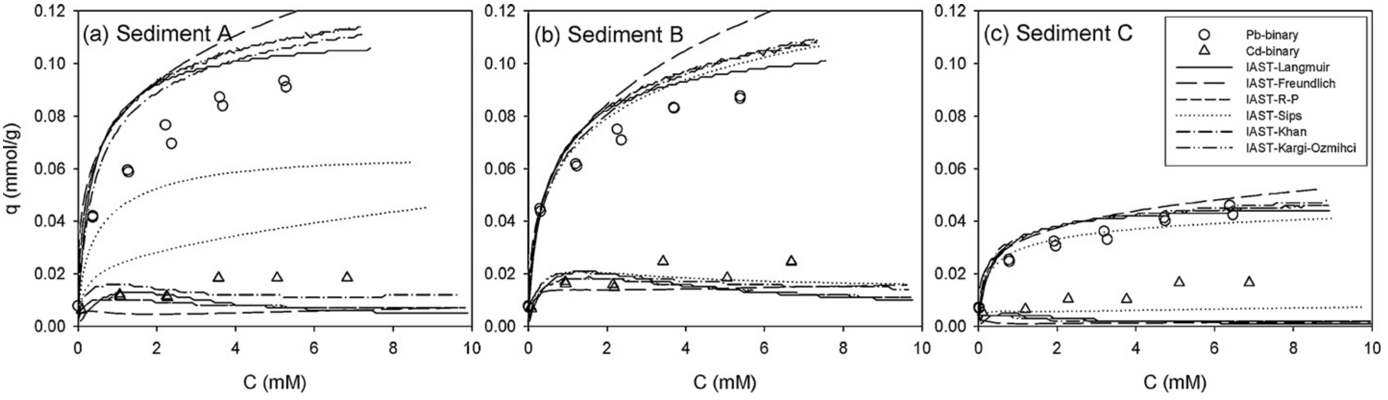

Fig. 10. Bi-solute competitive adsorption of Pb and Cd at pH 5.5. Lines represent IAST predictions coupled to the single-solute adsorption models.

Table 12
R^2 and SSE values for bi-solute competitive adsorption predictions from IAST coupled to single-solute adsorption model at pH 4.5 and 5.5, respectively.

pH	Sediment	Sorption model	R^2 (Pb/Cd)	SSE (Pb/Cd)
4.5	A	Freundlich	0.9971/0.3696	0.0001/0.0015
		Langmuir	0.9865/0.5972	0.0002/0.0010
		Sips	0.9972/0.4318	0.0001/0.0014
		R–P	0.9965/0.5041	0.0001/0.0012
		Kargi–Ozmıhci	0.9968/0.4318	0.0001/0.0014
		Khan	0.9980/0.4190	0.0000/0.0014
4.5	B	Freundlich	0.9946/0.7341	0.0001/0.0009
		Langmuir	0.9770/0.7607	0.0004/0.0007
		Sips	0.9851/0.7840	0.0003/0.0007
		R–P	0.9821/0.8342	0.0003/0.0006
		Kargi–Ozmıhci	0.9850/0.7880	0.0003/0.0008
		Khan	0.9855/0.8084	0.0003/0.0006
4.5	C	Freundlich	0.9681/0.2953	0.0002/0.0011
		Langmuir	0.9494/0.4548	0.0003/0.0011
		Sips	0.9621/0.3150	0.0002/0.0011
		R–P	0.9531/0.3705	0.0003/0.0010
		Kargi–Ozmıhci	0.9578/0.3150	0.0002/0.0011
		Khan	0.9566/0.3152	0.0002/0.0011
5.5	A	Freundlich	0.8948/0.5515	0.0028/0.0006
		Langmuir	0.9358/0.7832	0.0017/0.0004
		Sips	0.9213/0.7143	0.0021/0.0004
		R–P	0.9080/-	0.0024/0.0016
		Kargi–Ozmıhci	0.9224/0.7309	0.0020/0.0004
		Khan	0.9496/0.8702	0.0013/0.0002
5.5	B	Freundlich	0.9395/0.8861	0.0015/0.0002
		Langmuir	0.9809/0.8811	0.0005/0.0003
		Sips	0.9734/0.8986	0.0007/0.0002
		R–P	0.9832/0.9370	0.0004/0.0001
		Kargi–Ozmıhci	0.5274/0.8960	0.0012/0.0002
		Khan	0.9768/0.9158	0.0006/0.0002
5.5	C	Freundlich	0.9693/0.2027	0.0002/0.0007
		Langmuir	0.9770/0.2815	0.0001/0.0007
		Sips	0.9784/0.3274	0.0001/0.0006
		R–P	0.9925/0.7049	0.0000/0.0002
		Kargi–Ozmıhci	0.9788/0.3254	0.0001/0.0006
		Khan	0.9766/0.3064	0.0001/0.0006

few cases. However, the predictions for Cd in Sediment C for both pHs 4.5 and 5.5 were not successful.

4. Conclusions

The sorptions of Pb and Cd onto sediments have been studied using single- and bi-solute systems. In single-solute sorption, the sorption affinity of heavy metals onto sediments was in the order of Sediment B ≈ Sediment A > Sediment C for Pb and Sediment B > Sediment A > Sediment C for Cd, respectively. Generally the sorption affinity of Pb and Cd at pH 5.5 was higher than that at pH 4.5. Several sorption models such as Freundlich, Langmuir, Dubinin–Radushkevich, Sips, Redlich–Peterson, Kargi–Ozmıhci, and Khan models were fitted to the single-solute sorption data well. Generally three-parameter models (Sips, Redlich–Peterson, Kargi–Ozmıhcı, and Khan models) fitted better than the two-parameter models (Freundlich, Langmuir, and Dubinin–Radushkevich models). Competition between the solutes in bi-solute sorption reduced the sorbed amount of each solute compared with that in the single-solute system. Bi-solute competitive sorptions were analyzed by the Langmuir model. Sediments with higher pH, CEC and BET surface area had higher sorption capacity as estimated by the maximum sorption capacity (q_{mL}) of the Langmuir model. All sediments exhibited higher sorption capacity for Pb than Cd and Cd sorption was more affected than that of Pb in the bi-solute competitive system. The Langmuir binding strength parameter (b) of Pb was always greater than that of Cd. However, the b values tended to increase as a result of the simultaneous presence of both metals indicating competition for sorption sites decreasing the retention of both metals on specific sorption sites in sediments. The competitive Langmuir model (CLM) and ideal adsorbed solution theory (IAST) coupled to the single-solute sorption models predicted the Pb sorption in bi-solute competitive sorption data successfully but not the Cd sorption. Our results demonstrate that the single- and bi-solute competitive sorptions of Pb and Cd highly depend on sediment properties such as CEC and BET surface area.

Acknowledgement

The financial support of this work was provided by grant No. R01-2003-000-10593-0 from Korea Science and Engineering Foundation (KOSEF).

References

[1] J.M. Rodríguez-Maroto, R.A. García-Delgado, C. Gómez-Lahoz, C. Vereda-Alonso, F. García-Herruzo, M.P. Pérez Muñoz, Competitive retention of lead and cadmium on an agricultural soil, Environ. Monit. Assess. 89 (2003) 165–177.

[2] S. Serrano, F. Garrido, C.G. Campbell, M.T. Garcia, Competitive adsorption of cadmium and lead in acid soils of Central Spain, Geoderma 124 (2005) 91–104.

[3] R. Segura, V. Arancibia, M.C. Zúñiga, P. Pastén, Distribution of copper, zinc, lead and cadmium concentrations in stream sediments from the Mapocho River in Santiago, Chile, J. Geochem. Explor. 91 (2006) 71–80.

[4] T.H. Christensen, Cadmium soil sorption at low concentrations, II: reversibility, effect of changes in solute composition, and effect of soil aging, Water Air Soil Pollut. 21 (1984) 115–125.

[5] F. Wang, J. Chen, Relation of sediment characteristics to trace metal concentrations: a statistical study, Water Res. 34 (2000) 694–698.

[6] S. Lofts, E. Tipping, Solid-solution metal partitioning in the Humber rivers: application of WHAM and SCAMP, Sci. Total Environ. 251 252 (2000) 381–399.

[7] R.D. Harter, Competitive sorption of cobalt, copper and nickel ions by a calcium-saturated soil, Soil Sci. Soc. Am. J. 56 (1992) 444–449.

[8] H.A. Elliott, M.R. Liberati, C.P. Huang, Competitive adsorption of heavy metals by soils, J. Environ. Qual. 15 (1986) 214–219.

[9] J.C. Echeverria, M.T. Morera, C. Mazkiaran, J.J. Garrido, Competitive sorption of heavy metal by soils. Isotherms and fractional factorial experiments, Environ. Pollut. 101 (1998) 275–284.

[10] D.C.K. Ko, C.W. Cheung, K.K.H. Choy, J.F. Porter, G. McKay, Sorption equilibria of metal ions on bone char, Chemosphere 54 (2004) 273–281.

[11] A.M. Polcaro, M. Mascia, S. Palmas, A. Vacca, G. Tola, Competitive sorption of heavy metal ions by soils, Environ. Eng. Sci. 20 (2003) 607–616.

[12] G.W. Brümmer, J. Gerth, K.G. Tiller, Reaction kinetics of the adsorption and desorption of nickel, zinc, and cadmium by goethite I. Adsorption and diffusion of metals, J. Soil Sci. 39 (1988) 37–52.

[13] M.T. Pardo, Sorption of lead, copper, zinc and cadmium by soils: effect of nitriloacetic acid on metal retention, Commun. Soil Sci. Plant Anal. 31 (2000) 31–40.

[14] M.A. Trancoso, M.M. Correia dos Santos, M.L.S. Gonçalves, Lead sorption to selected Portuguese soils, Eur. J. Soil Sci. 58 (2007) 854–863.

[15] Q. Fan, J. He, H. Xue, C. Lu, Y. Liang, Saruli, Y. Sun, L. Shen, Competitive adsorption, release and speciation of heavy metals in the Yellow River sediments, China, Environ. Geol. 53 (2007) 239–251.

[16] D.C. Seo, K. Yu, R.D. DeLaune, Comparison of monometal and multimetal adsorption in Mississippi River alluvial wetland sediment: batch and column experiments, Chemosphere 73 (2008) 1757–1764.

[17] S.-H. Peng, W.-X. Wang, X. Li, Y.-F. Yen, Metal partitioning in river sediments measured by sequential extraction and biomimetic approaches, Chemosphere 57 (2004) 839–851.

[18] F. Bordas, A. Bourg, Effect of soild/liquid ratio on the remobilization of Cu, Pb, Cd, and Zn from polluted river sediment, modeling of the results obtained and determination of association constants between the metals and the sediment, Water Air Soil Pollut. 128 (2001) 391–400.

[19] S. Qiao, X. Hu, Use IAST with MPSD to predict binary adsorption kinetics on activated carbon, AIChE J. 46 (2000) 1743–1752.

[20] S. Sircar, Influence of adsorbate size and adsorbent heterogeneity on IAST, AIChE J. 41 (1995) 1135–1145.

[21] K. Wang, D.D. Do, Characterizing the micropore-size distribution of activated carbon using equilibrium data of many adsorbates at various temperatures, Langmuir 13 (1997) 6226–6233.

[22] S. Qiao, X. Hu, Effect of micropore size distribution induced heterogeneity on binary adsorption kinetics of hydrocarbons in activated carbon, Chem. Eng. Sci. 55 (2000) 1533–1544.

[23] S.K. Papageorgiou, F.K. Katsaros, E.P. Kouvelos, N.K. Kanellopoulos, Prediction of binary adsorption isotherms of Cu^{2+}, Cd^{2+} and Pb^{2+} on calcium alginate beads from single adsorption data, J. Hazard. Mater. 162 (2009) 1347–1354.

[24] Z. Yu, S. Peldszus, P.M. Huck, Adsorption characteristics of selected pharmaceuticals and an endocrine disrupting compound—Naproxen, carbamazepine and nonylphenol—on activated carbon, Water Res. 42 (2008) 2873–2882.

[25] M.A. Monsalvo, A.A. Shapiro, Modeling adsorption of binary and ternary mixtures on microporous media, Fluid Phase Equilib. 254 (2007) 91–100.

[26] U.S. EPA, Method 9081: Cation-Exchange Capacity (Sodium Acetate), Test Methods for the Evaluation of Solid Waste: Laboratory Manual Physical Chemical Methods. SW 846, USEPA, Office of Solid Waste, Washington, DC, 2003.

[27] U.S. EPA, Method 3051: Microwave assisted Acid Digestion of Sediments, Sludges, Soils, and Oils, Test Methods for the Evaluation of Solid Waste: Laboratory Manual Physical Chemical Methods. SW 846, USEPA, Office of Solid Waste, Washington, DC, 2003.

[28] D.G. Strawn, D.L. Sparks, Effects of soil organic matter on the kinetics and mechanisms of Pb(II) adsorption and desorption in soil, Soil Sci. Soc. Am. J. 64 (2000) 144–156.

[29] M.Y. Kwak, W.S. Shin, S.-O. Ko, J. Park, Y.K. Jeong, Modeling on the adsorption kinetics of lead and cadmium onto natural sediments, Korean J. Limnol. 39 (2006) 450–461.

[30] Y. Xu, T. Boonfueng, L. Axe, S. Maeng, T. Tyson, Surface complexation of Ph(II) on amphorous iron oxide and manganese oxide: spectroscopic and time studies, J. Colloid Interf. Sci. 299 (2006) 28–40.

[31] M.M. Dubinin, The potential theory of adsorption of gases and vapors for adsorbents with energetically non-uniform surface, Chem. Rev. 60 (1960) 235–266.

[32] S. Kundu, A.K. Gupta, Arsenic adsorption onto iron oxide-coated cement (IOCC): regression analysis of equilibrium data with several isotherm models and their optimization, Chem. Eng. J. 122 (2006) 93–106.

[33] O. Redlich, D.L. Peterson, A useful adsorption isotherm, J. Phys. Chem. 63 (1959) 1024–1026.

[34] V.C. Srivastava, I.D. Mall, I.M. Mishra, Equilibrium modelling of single and binary adsorption of cadmium and nickel onto bagasse fly ash, Chem. Eng. J. 117 (2006) 79–91.

[35] F. Kargi, S. Ozmıhcı, Biosorption performance of powdered activated sludge for removal of different dyestuffs, Enzyme Microb. Technol. 35 (2004) 267–271.

[36] A.R. Khan, R. Ataullah, A. Al-Haddad, Equilibrium adsorption studies of some aromatic pollutants from dilute aqueous solutions on activated carbon at different temperatures, J. Colloid Interf. Sci. 194 (1997) 154–165.

[37] C.J. Radke, J.M. Prausnitz, Thermodynamics of multi-solute adsorption from dilute liquid solutions, AIChE J. 18 (1972) 761–768.

[38] C.Y. Yen, P.C. Singer, Competitive adsorption of phenols on activated carbon, J. Environ. Eng. 110 (1984) 976–989.

[39] W. Stumm, Chemistry of the Solid-Water Interface, John Wiley and Sons, New York, 1992.

[40] C.H. Giles, D. Smith, A. Huitson, A general treatment and classification of the solute adsorption isotherm. I. Theoretical, J. Colloid Interf. Sci. 47 (1974) 755–765.

[41] D. Suteu, D. Bilba, F. Dan, Synthesis and characterization of polyamide powders for sorption of reactive dyes from aqueous solutions, J. Appl. Polymer Sci. 105 (2007) 1833–1843.

[42] N. Hilal, G. Busca, F. Rozada, N. Hankins, Use of activated carbon to polish effluent from metalworking treatment plant: comparison of different streams, Desalination 185 (2005) 297–306.

[43] G. McKay, H.S. Blair, J.R. Gardner, Adsorption of dyes on chitin. I. Equilibrium studies, J. Appl. Polymer Sci. 27 (1982) 3040–3057.

[44] R. Han, P. Han, Z. Cai, Z. Zhao, M. Tang, Kinetics and isotherms of Neutral Red adsorption on peanut husk, J. Environ. Sci. 20 (2008) 1035–1041.

[45] R. Apiratikul, P. Pavasant, Batch and column studies of biosorption of heavy metals by Caulerpa lentillifera, Bioresource Technol. 99 (2008) 2766–2777.

[46] A. Sarı, M. Tuzen, Kinetic and equilibrium studies of biosorption of Pb(II) and Cd(II) from aqueous solution by macrofungus (Amanita rubescens) biomass, J. Hazard. Mater. 164 (2009) 1004–1011.

[47] H. Arslanoglu, H.S. Altundogan, F. Tumen, Heavy metals binding properties of esterified lemon, J. Hazard. Mater. 164 (2009) 1406–1413.

[48] R. Apiratikula, P. Pavasant, Sorption of Cu^{2+}, Cd^{2+}, and Pb^{2+} using modified zeolite from coal fly ash, Chem. Eng. J. 144 (2008) 245–258.

[49] P.C. Gomes, M.P.F. Fontes, A.G. da Silva, E.S. Mendoca, A.R. Netto, Selectivity sequence and competitive adsorption of heavy metals by Brazilian soils, Soil Sci. Soc. Am. J. 65 (2001) 1115–1121.

[50] R. Adhikari, M.V. Singh, Adsorption characteristics of lead and cadmium in some soils of India, Geoderma 114 (2003) 81–92.

[51] M.P.F. Fontes, P.C. Gomes, Simultaneous competitive adsorption of heavy metals by the mineral matrix of tropical soils, Appl. Geochem. 18 (2003) 795–804.

[52] I. Christl, R. Kretzschmar, Competitive adsorption of copper and lead at the oxide–water interface: implications for surface site density, Geochim. Cosmochim. Acta 63 (1999) 2929–2938.

[53] P. Trivedi, L. Axe, J. Dyer, Adsorption of metal ions onto goethite: single-adsorbate and competitive systems, Colloids Surf. A: Physicochem. Eng. Aspects 191 (2001) 107–121.

[54] U.K. Saha, S. Taniguchi, K. Sakurai, Simultaneous adsorption of cadmium, zinc, and lead on hydroxyalumium- and hydroxyaluminosilicate-montmorillinite complexes, Soil Sci. Soc. Am. J. 66 (2002) 117–128.

[55] M.E. Mesquita, J.M. Viera e Silva, Preliminary study of pH effect in the application of Langmuir and Freundlich isotherms to Cu-Zn competitive adsorption, Geoderma 106 (2002) 219–234.

[56] D.L. Sparks, Environmental Soil Chemistry, 2nd ed., Academic Press, San Diego, CA, 2002.

[57] W.H. Van Riemsdijk, G.H. Bolt, L.K. Koopel, J. Blaakmeer, Electrolyte adsorption on heterogeneous surfaces: adsorption models, J. Colloid Interf. Sci. 109 (1985) 219–228.